Journal of
Materials in Life Sciences

Vol. 4 No. 2 (2025)

Full Paper

Anticancer Activity of Curcumin-Loaded CMC Hydrogel Combined with Near-Infrared Radiation on MCF-7 Breast Cancer Cells

Nurfarrahhin Rosle[a], Ong Wan Jun[a], Khairunadwa Jemon[a,b], Wan Fatin Amira Wan Mohd Zawawi[a,b*]

[a] Department of Biosciences, Faculty of Science, Universiti Teknologi Malaysia, 81310, Johor, Malaysia.
[b] Cancer and Infectious Diseases Group, Health and Wellness Research Alliance, Universiti Teknologi Malaysia, 81310, Johor, Malaysia.

Article history
Received
4 August 2025
Revised
13 September 2025
Accepted
22 September 2025
Published online
31 November 2025

*Corresponding author
wanfatinamira@utm.my

Abstract

Curcumin, a bioactive compound derived from *Curcuma longa*, has demonstrated anticancer properties against various cancers, including breast cancer. However, its clinical potential is often limited by poor bioavailability and rapid degradation. To address these challenges, a hydrophilic system, such as a hydrogel, was necessary to enhance its efficiency. Hydrogel drug delivery systems derived from carboxymethyl cellulose (CMC) are gaining attention for their affordability, water solubility, and controlled drug release. Additionally, near-infrared radiation (NIR) has emerged as a non-invasive strategy to enhance drug delivery efficacy through localized hyperthermia. In this study, a CMC hydrogel was synthesized from oil palm empty fruit bunch (OPEFB) and characterized by FT-IR, XRD, and SEM to assess chemical modifications. Curcumin was incorporated into the hydrogel matrix via physical adsorption, and the optimal curcumin concentration was determined from drug release kinetics. The anticancer activity of the Cur-loaded CMC hydrogel was then evaluated against MCF-7 breast cancer cells using the MTT assay, both as a standalone treatment and in combination with near-infrared radiation. Results demonstrated that the Cur-CMC hydrogel effectively enhanced curcumin delivery to target cells, as evidenced by a significant reduction in cell viability compared with free curcumin. While the addition of NIR did not lead to a marked increase in cytotoxicity, it represents a feasible approach for future exploration in enhancing localized treatment strategies.

Keywords: curcumin; anticancer; hydrogel; carboxymethyl cellulose (CMC); near infrared radiation (NIR)

1.0 INTRODUCTION

According to the International Agency for Research on Cancer (IARC), breast cancer is recognized as the leading malignancy among women worldwide [1]. Surgery remains the primary treatment for early breast cancer; however, most patients undergo systemic therapies post-surgery to reduce the risk of recurrence or metastasis [2].

Curcumin (Cur), a natural compound derived from the rhizome of *Curcuma longa*, has been shown to inhibit various cancers by regulating cancer cell proliferation, metastasis, and angiogenesis [3]. Curcumin targets signalling pathways associated with cancer therapy and inhibits breast cancer cell proliferation through multiple molecular mechanisms, including p53-dependent apoptosis, alterations in phosphatidylinositol-3-kinase (PI3K) expression, Ras, Wnt/β-catenin, and

down-regulation of transcription factors [4]. Despite its therapeutic potential, curcumin's native hydrophobicity and poor bioavailability have restricted its clinical application. With the recent advent of nanotechnology, various curcumin formulations have been developed to overcome the limitations of native curcumin and enhance its therapeutic activity through improved cellular uptake [5]. Some curcumin nanoparticles developed with improved bioavailability were in the form of micelles, polymer and solid lipid nanoparticles [6].

Hydrogels are 3D polymeric networks that have emerged across biomedical application systems due to their hydrophilicity, biodegradability, biocompatibility, and non-toxicity [7]. Their tunable swelling behaviour and controlled drug release capacity make them ideal carriers for drug delivery [8]. Recent studies have explored various hydrogel systems, such as injectable liposome hydrogel, self-assembled peptide hydrogel and polymer-based hydrogel for curcumin delivery in the treatment of breast cancer, head and neck tumours, and colon cancer, respectively [9]. Among natural polymers, cellulose and its derivatives, particularly carboxymethyl cellulose (CMC), have attracted significant attention due to their low cost, low toxicity, good biocompatibility, water solubility, and ability to provide controlled drug release [10].

To further enhance the therapeutic efficacy of drug-loaded hydrogels, hyperthermia (HT) has become a complementary treatment modality. HT involved the application of localized heat, typically ranging from 40℃ to 43℃, to enhance anticancer treatment outcomes. It is frequently employed alongside radiotherapy and chemotherapy for recurrent breast cancer, cervical carcinoma, bladder cancer, melanoma, and soft tissue sarcoma [11]. HT has been reported to increase vascular permeability and stromal blood flow, thereby improving drug uptake in tumour tissues [12]. HT accelerates drug release from the hydrogel and increases cancer cells' susceptibility to cytotoxic effects. HT can also stimulate immunogenic cell death, enhancing antitumor immune responses. When combined with sustained drug release, cancer cells become more susceptible to cytotoxic effects. Together, this combination can enhance apoptosis and inhibit tumour proliferation more effectively than either treatment alone.

In parallel with efforts to develop an advanced drug delivery system, there is a growing emphasis on using sustainable, renewable resources for biomaterial development. Malaysia, a prominent global oil palm producer, generates substantial biomass waste, particularly oil palm empty fruit bunches (OPEFB), posing challenges in its disposal [13,14]. It is typically underutilized, being discarded, burned, or composted due to limited current economic value [14]. However, due to its high cellulose content, OPEFB presents a valuable and sustainable resource for the production of cellulose-based hydrogel [14]. Therefore, this study aims to develop a curcumin-loaded CMC hydrogel derived from OPEFB biomass as a sustainable biomaterial for drug delivery with potential applications in breast cancer therapy. By integrating this hydrogel with NIR-induced mild HT, the approach seeks to enhance targeted curcumin delivery, offering a preliminary strategy to improve cancer therapy outcomes while providing foundational data for future optimization studies.

2.0 EXPERIMENTAL

2.1 Materials

OPEFB was collected from the Southern Malay Palm Oil Mill in Kluang, Johor, Malaysia. Sodium Monochloroacetate (SMCA; Acros organic, Belgium), Methanol (100%), Sodium Hydroxide (NaOH, 99%), Glacial Acetic Acid (99.8%), Isopropanol (IPA, 98%) and Toluene were all purchased from Merck (USA), Absolute Ethanol (99.7%) (Hayman limited, USA), Calcium Chloride ($CaCl_2$), Sodium Chlorite ($NaClO_2$) and Curcumin were all purchased from Sigma Aldrich (USA), Dulbecco'sModified Eagle Medium/Nutrient (DMEM) (Gibco, Malaysia), phosphate buffered saline (Oxoid, Malaysia), MCF-7 cells, DMSO (Fisher Chemical, Malaysia) were used in this study. The analytical-grade chemicals used in this study were not further purified.

2.2 Preparation of Materials

2.2.1 Extraction of Cellulose

The preparation of 20% CMC hydrogel involved several steps. Cellulose was extracted from OPEFB, converted to CMC, and used to prepare a 20% CMC hydrogel. Cellulose was extracted according to the method described in Salleh et al. [15]. The sample was ground and washed with distilled water 3 times to remove impurities, then dried in an oven at 70°C for 24 hours. Next, the dried sample was mixed with toluene and ethanol at a 2:1 ratio for 6 hours, then further dried for 24 hours at 70°C in an oven. Following that, the sample was digested with 1.0 M NaOH for 4 hours at 80°C and washed with distilled water until the pH reached 7. It was then left to dry overnight at 70°C. The following day, the sample was mixed with 10% acetic acid and 1.3% sodium chlorite in a 1:1 ratio for 4 hours at 80°C. Then, it was washed with 0.1 M NaOH, followed by distilled water until the pH reached 7. The sample was dried for 24 hours at 70°C.

2.2.2 Preparation of CMC

The CMC from cellulose-derived OPEFB was prepared using the procedures outlined by Tuan Mohamood et al. [14]. OPEFB cellulose was mixed with 10ml of 30% NaOH solution dropwise and followed by 100ml of isopropanol at room temperature for an hour. Next, sodium monochloroacetic acid (SMCA) was added to complete the carboxymethylation reaction. The reaction was set to continue for 3 hours at 45°C. After the filtration process, the sample was immersed in 300ml of methanol overnight.

Then, the glacial acetic acid was used to neutralize the sample. The sample was sieved and washed three times with 70% ethanol, followed by 99.7% ethanol. The sample was then oven-dried for 24 hours at 60°C.

2.2.3 Preparation of 20% CMC Hydrogel

20% CMC was mixed with 1% CaCl2 solution and stirred until a paste-like CMC-$CaCl_2$ solution was obtained. The CMC-$CaCl_2$ paste was left to crosslink in a petri dish at room temperature for 24 hours.

2.3 Characterization of Materials

Fourier-transform infrared spectroscopy (FTIR) was used to detect functional groups in OPEFB cellulose, CMC, and a 20% CMC hydrogel. Next, X-ray diffraction (XRD) was used to observe the crystallinity of OPEFB cellulose, CMC, and 20% CMC hydrogel. Lastly, scanning electron microscopy (SEM) was used to study the surface morphology of OPEFB cellulose, CMC, and 20% CMC hydrogel.

2.4. Loading and Release Capacity of Cur in Cur-Loaded CMC Hydrogel

2.4.1. The Curcumin Loading Capacity

Curcumin loading into a 20% CMC hydrogel was performed according to the method established by Ravindra et al. [16]. Three different concentrations of Cur were used in this experiment: 1 g/L, 2.5 g/L, and 5 g/L. Then, 20% CMC hydrogel was swelled in 20 mL of Cur/ethanol solution at various concentrations at room temperature for 24 hours in the dark. After that, the CMC hydrogel was removed from the Cur/ethanol solution and washed three times with 20 mL of distilled water to remove excess curcumin from its surface. Finally, the Cur-loaded CMC hydrogel was placed in a petri dish covered with aluminum foil and further dried at room temperature in the dark for 48 hours. The loading capacity of hydrogels will be determined by using this formula:

$$\text{Loading Capacity (\%)} = (Wa - Wi) / Wa \times 100\% \quad (2.1)$$

where, Wi and Wa represent the initial weight of dried hydrogels and the weight of dried hydrogels after being immersed in Cur/ethanol solution, respectively.

2.4.2. The Curcumin Release Capacity

The Cur release capacity was conducted, and the protocol was adjusted based on the procedure established by Huang et al. [17]. The Cur-loaded CMC hydrogel was soaked in 50ml of pure ethanol medium at 37°C. During the initial 2 hours, a 500 µL aliquot of the solution was pipetted out and analyzed by using a UV-visible spectrometer at 420nm at 10-minute intervals. Simultaneously, 500 µL of fresh pure ethanol solution was added to replenish the withdrawn solution for absorbance measurement. Then, the process in step 2 was repeated every 2 hours for 24 hours. Following that, readings were recorded every 12 hours for the next 24 hours. The released amount was determined by calculating the drug concentration in a pure ethanol medium and comparing it to the standard curve.

2.5. Cytotoxicity Assay

Cell viability was assessed using the MTT assay to detect viable cells in the wells. 100 µL of 1×10 ^5 MCF-7 cells were seeded in 96-well plates and incubated in a 5% CO_2 incubator at 37°C for 24 hours. The cells were subjected to four treatment groups: free curcumin, Cur-loaded CMC hydrogel alone, near-infrared radiation alone, and Cur-loaded CMC hydrogel with near-infrared radiation. An incubation time of 24 hours was chosen to determine the delivery efficiency of Cur loaded on CMC hydrogel before the MTT assay was performed. For treatment groups involving near-infrared radiation, MCF-7 cells were irradiated at 1.5 W/cm^2 using an external wIRA radiator (wIRA, Hydrosun 750, Germany) for 5 minutes. An incubation time of 24 hours was selected as optimal before the MTT assay. Untreated cells were selected as the negative control group in both experiments.

For the MTT assay, 25 µL of 5 mg/mL MTT solution in PBS was added to each well, and the plate was incubated for 3 hours at 37°C. After discarding the supernatant, the formazan crystals were dissolved by adding 100 µL of DMSO solution to each well. The plate was incubated at 37°C in a 5% CO2 atmosphere for 20 minutes. Finally, a microplate reader was used to measure the optical density at 570nm. In all experiments, cell viability was measured as the absorbance of the control wells containing only untreated cells. Experiments were conducted in triplicate (n=3 per group). Statistical analysis was done by using one-way ANOVA followed by Tukey's post hoc test in GraphPad Prism version 10.2.2. Differences were considered statistically significant at $p < 0.05$. The cell viability was then calculated using the equation:

$$\text{Cell viability (\%)} = \text{abs treated group} / \text{abs control group} \times 100\% \quad (2.2).$$

3.0 RESULTS AND DISCUSSION

3.1 Characterization of OPEFB Cellulose, CMC and 20% CMC Hydrogel

3.1.1 Fourier Transform-Infrared Spectroscopy (FT-IR)

Figure 1 represents the FTIR spectra of OPEFB cellulose, CMC, and the 20% CMC hydrogel. The presence of main polysaccharide bands, such as -OH stretching at 3333 cm^{-1} and -CH stretching at 2893 cm^{-1}, confirms the cellulose nature of the OPEFB material [14]. The intense C-O stretching vibration at 1030 cm^{-1}, associated with the pyranose ring, is also observed, further supporting the cellulose structure [14]. The successful synthesis of CMC from OPEFB cellulose is indicated by the appearance of new absorption peaks at 1589 cm^{-1} and 1414 cm^{-1}, attributed to the stretching of the carboxyl group ($-COO^-$), particularly after treatment with NaOH. Comparison of the CMC and 20% CMC hydrogel spectra reveals a slight decrease in wavenumber at 1587 cm^{-1} and an increase at 1417 cm^{-1}. These are likely attributed to the substitution of sodium ions by calcium ions during the ionic cross-linking process to form the hydrogel [18]. Collectively, these FTIR results confirm the successful extraction of cellulose from OPEFB and its subsequent conversion into a 20% CMC hydrogel.

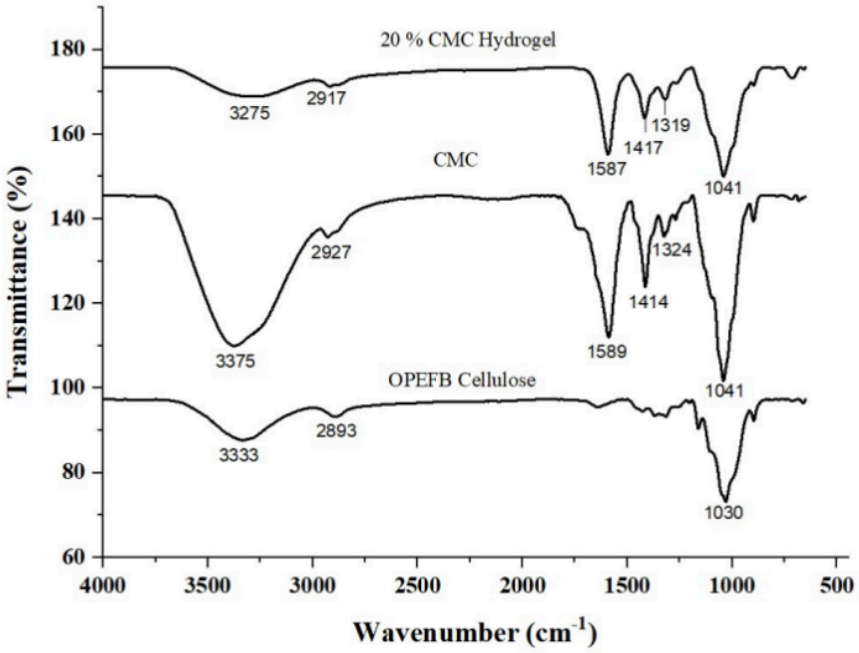

Figure 1 : FT-IR spectra of OPEFB cellulose, CMC, and 20% CMC hydrogel. The characteristic peaks at 3333 cm^{-1} (-OH stretching), 2893 cm^{-1} (-CH stretching), and 1030 cm^{-1} (C–O stretching of the pyranose ring) confirm the cellulose structure of OPEFB. New absorption peaks at 1589 cm^{-1} and 1414 cm^{-1} correspond to the carboxyl ($-COO^-$) groups, suggesting successful carboxymethylation. Shifts in peak positions at 1587 cm^{-1} and 1417 cm^{-1} in the hydrogel spectrum reflect ionic cross-linking with calcium ions. Spectra are offset vertically for clarity.

3.1.2 X-Ray Diffraction

As depicted in Figure 2, the OPEFB cellulose diffractogram exhibited characteristic peaks indicative of both amorphous and crystalline phases, notably at 2θ = 15°- 16° and 2θ = 21°- 22°. The structure changes after modification of OPEFB cellulose to CMC, as a significant number of the OPEFB cellulose peaks had been transformed to the amorphous phase. This loss of crystallinity is attributed to the substitution of hydroxyl groups within the cellulose crystallites during the carboxymethylation process, which also enhances water solubility [14, 19]. The 20% CMC hydrogel also exhibited a fully amorphous structure, as evidenced by the absence of sharp diffraction peaks. This is likely due to the extensive cross-linking induced by Ca^{2+} ions, which restricted the flexibility of the cellulose chains. This further suggests that the 20% CMC hydrogel was completely converted to an amorphous state following carboxymethylation and ionic cross-linking.

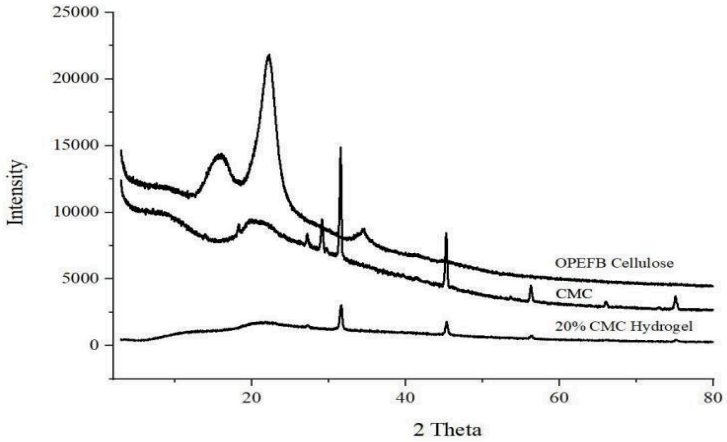

Figure 2 : XRD patterns of OPEFB cellulose, CMC, and 20% CMC hydrogel

3.1.3 Scanning Electron Microscopy (SEM)

Figure 3 shows an SEM micrograph of OPEFB cellulose, CMC, and 20% CMC hydrogel. In Figure 3, it can be observed that OPEFB cellulose exhibits a rough surface in fibre form, likely due to the use of strong chemicals and high temperatures during the extraction process to remove natural and artificial contaminants [14]. When compared to OPEFB cellulose, CMC has a smoother fibrous structure, due to the changes in cellulose crystallinity that facilitate the ability of the etherifying agent to modify the cellulose structure [19]. The freeze-dried 20% CMC hydrogel, however, presents inconsistently sized macropores. Variation in pore size in hydrogel may be related to differences in cross-linking density, leading to significantly greater or lesser water uptake before freeze-drying [14]. In addition, the presence of these macropores in the CMC hydrogel suggests enhanced matrix-water interactions, which may be beneficial for drug loading and release.

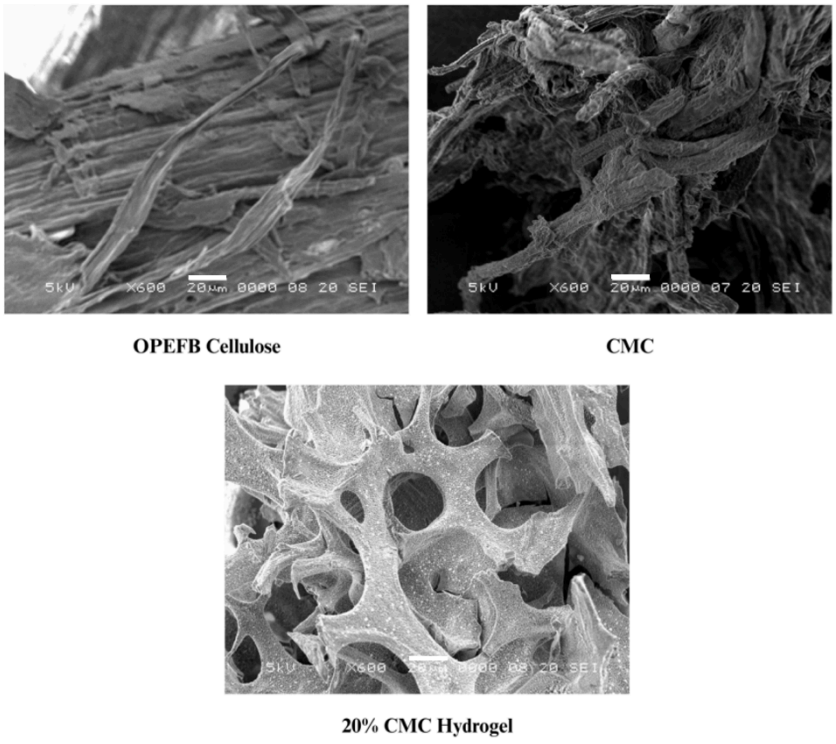

Figure 3 : SEM images of OPEFB cellulose, CMC and 20% CMC hydrogel at 600x magnification (Scale bar 20 µm). OPEFB cellulose shows rough fibrous morphology, CMC exhibits smoother fibres due to etherification, while the freeze-dried hydrogel displays irregularly sized macropores that support enhanced water absorption and drug delivery potential.

3.2 Loading and Release Capacity of Curcumin in Cur-Loaded CMC Hydrogel

3.2.1 The Curcumin Loading Capacity

The analysis was performed to assess the potential of CMC hydrogel as a drug delivery system by assessing its loading capacity. Based on Figure 4, across all 20% CMC hydrogels tested, loading capacities ranged from 80% to 90%. It is suggested that the observed differences in loading capacity may be due to variations in pore size within the hydrogel. Since there are no significant differences in the loading results across all concentrations tested, the Cur release study was conducted to observe sustained Cur release, thereby facilitating the identification of the optimal Cur concentration.

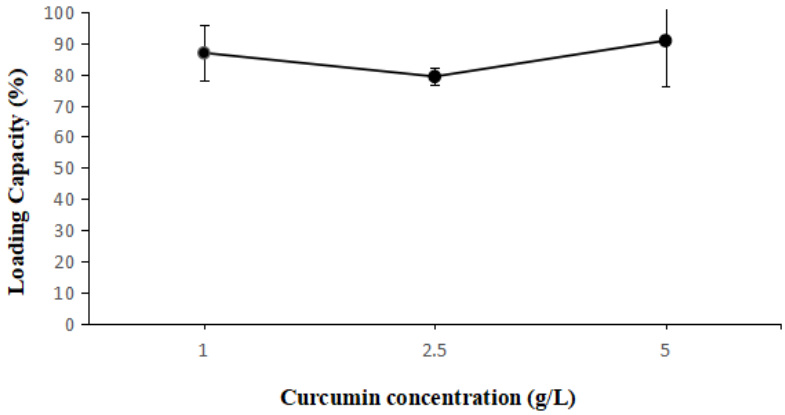

Figure 4: The drug loading capacity of the 20% CMC hydrogel in different Cur concentrations.

3.2.2 The Curcumin Release Capacity

The findings obtained from the drug release capacity of Cur-loaded CMC hydrogel are presented in Figure 5. The drug release pattern for all hydrogels loaded with different Cur concentrations can be categorized into two phases: an initial burst release and a prolonged sustained release phase. In contrast to other Cur concentrations, the Cur-loaded CMC hydrogels at 2.5 g/L show a more gradual, sustained release pattern for up to 48 hours. Although Cur-loaded CMC hydrogels at 5 g/L have the highest loading capacity, they exhibit unstable release over 12 to 24 hours. This may be due to a high Cur concentration during loading, which could cause saturation within the hydrogel. Consequently, it could lead to the blocking of pores during the drug release phase and further cause unstable drug release patterns.

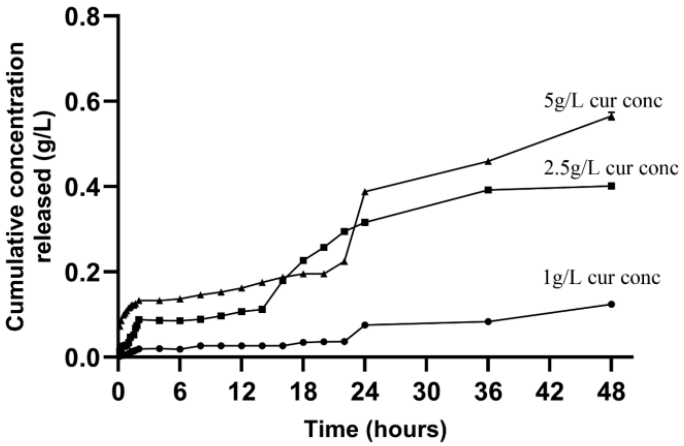

Figure 5: The drug release capacity of curcumin-loaded CMC hydrogel in pure ethanol solution in different Cur concentrations.

The experimental data were also analyzed using various kinetic models, including Higuchi, first-order, and zero-order, to determine the mechanism of Cur release from Cur-loaded CMC hydrogel. The model that best fits the Cur release pattern was selected based on the highest coefficient of correlation (R^2). Based on Table 1, the kinetic modelling indicated that the 2.5

g/L curcumin concentration followed a zero-order release profile, indicating a predictable, sustained release. It is beneficial for anti-cancer therapy, as it can help minimize the risks of under- or overdosing, reduce systemic toxicity, and enhance treatment efficacy by providing continuous drug exposure to cancer cells over a defined period [20]. This finding validates the potential of the 2.5 g/L formulation for controlled delivery of curcumin over an extended period. This suggests that the Cur-loaded CMC hydrogels at a 2.5 g/L Cur concentration exhibit properties of a good drug delivery system and could be beneficial for anticancer therapy.

Table 1: Drug release kinetics for Cur release from the Cur-loaded CMC hydrogel

Cur concentration	(R^2)		
	Zero-Order Model	First Order Model	Higuchi model
1 g/L	0.9010	0.7294	0.7840
2.5 g/L	0.9256	0.7302	0.9017
5 g/L	0.9027	0.9145	0.7627

3.3. Cytotoxicity Assay

The cytotoxic effects of the Cur-loaded CMC hydrogel, alone and in combination with near-infrared radiation (NIR), were evaluated in MCF-7 cells using an MTT assay, with an untreated control serving as a baseline for cell viability (Figure 6). All experiments were performed in triplicate (n=3 per group), and statistical analysis was conducted using one-way ANOVA followed by Tukey's post hoc test. Free curcumin did not significantly inhibit cell proliferation, whereas the Cur-loaded CMC hydrogel exhibited higher cytotoxicity (****p <0.0001), indicating that encapsulation within a hydrophilic hydrogel overcomes curcumin's poor solubility and bioavailability [21]. The swelling capacity of CMC, a water-soluble cellulose derivative synthesized via carboxymethylation, facilitates drug-controlled release by absorbing aqueous fluid within its macropores [22]. The most substantial cytotoxic effect was observed in the combined treatment group, in which MCF-7 cells treated with both the Cur-loaded CMC hydrogel and NIR exhibited a 92.7% reduction in cell viability (****p <0.0001). This outcome was significantly lower than with NIR alone (96.1% viability, p > 0.05) or with the Cur-loaded CMC hydrogel alone (17% viability, ****p < 0.0001). This enhancement is likely due to NIR increasing the fluidity of the phospholipid bilayer, thereby facilitating drug uptake [23], demonstrating the synergistic effect of NIR with hydrogel-based drug delivery.

The limited cytotoxicity observed with NIR alone suggests that the applied parameters (1.5 W/cm² for 5 minutes) were insufficient to induce significant therapeutic HT. Factors such as suboptimal irradiation intensity and duration, absence of photosensitizers, and limited heat retention in vitro may have contributed to this finding. Future optimization could involve higher irradiation intensities, longer exposure times, the incorporation of NIR-absorbing nanoparticles, and real-time temperature monitoring to maintain the therapeutic HT range (40–45°C). Despite these limitations, the observed synergy underscores the potential of NIR-assisted Cur-loaded hydrogel systems and provides a foundation for further parameter optimization. Cell viability was assessed using the MTT assay, and future studies may incorporate complementary methods, such as apoptosis assays, to corroborate these findings and strengthen the cytotoxicity assessment.

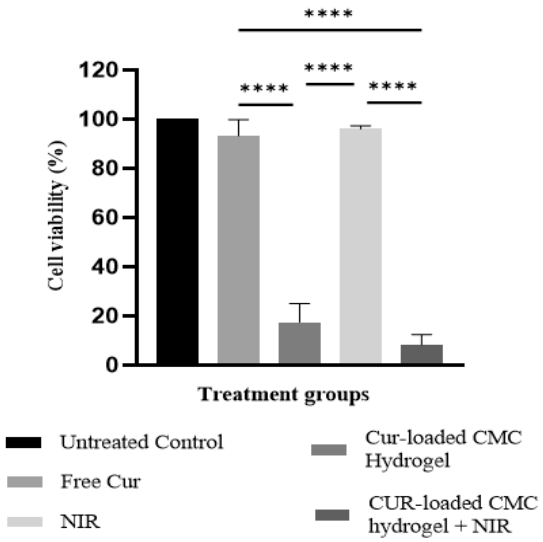

Figure 6 : The percentage of cell viability (mean ± SEM, n=3 per group) for untreated MCF-7 cells, treated with free curcumin, treated with Cur-loaded CMC hydrogel, MCF-7 cells irradiated using only NIR, and lastly a combination of Cur-loaded CMC hydrogel and NIR evaluated by MTT assay after 24 hours of incubation. Cell viability was

expressed relative to the untreated control (100%). Statistical analysis was performed using one-way ANOVA with Tukey's post hoc test (****p<0.0001).

4.0 CONCLUSION

In this study, a Cur-loaded CMC hydrogel synthesized from OPEFB was successfully developed and characterized, confirming carboxymethylation, crosslinking, and a macroporous structure. The optimal curcumin concentration (2.5 g/L) enabled sustained release for 48 hours. The hydrogel enhanced curcumin's cytotoxicity against MCF-7 cells, and its combination with NIR produced the lowest cell viability, demonstrating a synergistic anticancer effect. These results indicate that OPEFB-derived CMC hydrogel is a promising drug carrier for improving solubility, bioavailability, and targeted delivery of hydrophobic drugs, while NIR-induced hyperthermia can further enhance cytotoxicity by increasing cell membrane permeability. Future studies could focus on *in vivo* evaluation and optimization of NIR parameters to further improve therapeutic efficacy.

Acknowledgment

This research was funded by Universiti Teknologi Malaysia Encouragement Grant (31J29). The authors thanked the Faculty of Science, Universiti Teknologi Malaysia, and Southern Malay Palm Oil Mill for their full support throughout this study.

References

[1] World Health Organization. (2024, February 1). *Global cancer burden growing, amidst mounting need for services.* World Health Organization. Retrieved from https://www.who.int/news/item/01-02-2024-global-cancer-burden-growing--amidst-mounting-need-for-services
[2] Alkabban, F. M. (2022, September 26). *Breast cancer. StatPearls - NCBI Bookshelf.* Retrieved from https://www.ncbi.nlm.nih.gov/books/NBK482286/
[3 Wang, M. P., Jiang, S., Zhou, L., Yu, F., Ding, H., Li, P., Zhou, M., & Wang, K. (2019). Potential mechanisms of action of curcumin for cancer prevention: Focus on cellular signaling pathways and miRNAs. *International Journal of Biological Sciences, 15*(6), 1200–1214.
[4] Song, X., Zhang, M., Dai, E., & Wang, F. (2018). Molecular targets of curcumin in breast cancer (Review). *Molecular Medicine Reports.*
[5] Gera, M., Sharma, N., Ghosh, M., Huynh, D. L., Lee, S., Min, T., Kwon, T., & Jeong, D. S. (2017). Nanoformulations of curcumin: An emerging paradigm for improved remedial application. *Oncotarget, 8*(39), 66680–66698.
[6] Panda, A. K., Chakraborty, D., Sarkar, I., Khan, T., & Sa, G. (2017). New insights into therapeutic activity and anticancer properties of curcumin. *Journal of Experimental Pharmacology, 9*, 31–45.
[7] Nafo, W. (2023). *Hydrogel biomaterials for drug delivery: Mechanisms, design, and drugs.* IntechOpen eBooks.
[8] Lei, L., Bai, Y., Qin, X., Liu, J., Huang, W., & Lv, Q. (2022). Current understanding of hydrogel for drug release and tissue engineering. *Gels, 8*(5), 301.
[9] Madamsetty, V. S., Vazifehdoost, M., Alhashemi, S. H., Davoudi, H., Zarrabi, A., Dehshahri, A., Fekri, H. S., Mohammadinejad, R., & Thakur, V. K. (2023). Next-generation hydrogels as biomaterials for biomedical applications: Exploring the role of curcumin. *ACS Omega.*
[10] Peptu, C. A., Băcăiță, E. S., Savin, C., Luțcanu, M., & Agop, M. (2021). Hydrogels based on alginates and carboxymethyl cellulose with modulated drug release—An experimental and theoretical study. *Polymers, 13*(24), 4461.
[11] Crezee, J., Franken, N. A. P., & Oei, A. L. (2021). Hyperthermia-based anticancer treatments. *Cancers, 13*(6), 1240.
[12] Maurici, C. E., Colenbier, R., Wylleman, B., Brancato, L., Van Zwol, E., Van Den Bossche, J., Timmermans, J., Giovannetti, E., Da Cunha, M. S., & Bogers, J. (2022). Hyperthermia enhances the efficacy of chemotherapeutic agents in pancreatic cancer cell lines. *Biomolecules, 12*(5), 651.
[13] Ali, M. M., Muhadi, N. A., Hashim, N., Abdullah, A. F., & Mahadi, M. R. (2020). Pulp and paper production from oil palm empty fruit bunches: A current direction in Malaysia. *Journal of Agricultural and Food Engineering, 2*, 1–9.
[14] Tuan Mohamood, N. F., Abdul Halim, A. H., & Zainuddin, N. (2021). Carboxymethyl cellulose hydrogel from biomass waste of oil palm empty fruit bunch using calcium chloride as crosslinking agent. *Polymers, 13*(23), 4056.
[15] Salleh, N., & Salamun, N. (2022). *Extraction and characterization of cellulose derived from oil palm empty fruit bunch.* (Vol. 14). [Publication details incomplete].
[16] Ravindra, S., Mulaba-Bafubiandi, A. F., Rajinikanth, V., Varaprasad, K., Narayana Reddy, N., & Mohana Raju, K. (2012). Development and characterization of curcumin loaded silver nanoparticle hydrogels for antibacterial and drug delivery applications. *Journal of Inorganic and Organometallic Polymers and Materials, 22*(6), 1254–1262.
[17] Huang, B., Liu, M., & Zhou, C. (2017). Cellulose–halloysite nanotube composite hydrogels for curcumin delivery. *Cellulose, 24*(7), 2861–2875.
[18] Fitrah, N., Nan, C., Zainuddin, N., & Ahmad, M. (2019). Preparation and swelling study of CMC hydrogel as potential superabsorbent. *Pertanika Journal of Science & Technology, 27*(1), 489–498.
[19] Parid, D. M., Abd Rahman, N. A., Baharuddin, A. S., Mohammed, M. A. P., Johari, A. M., & Razak, S. Z. A. (2018). Synthesis and characterization of carboxymethyl cellulose from oil palm empty fruit bunch stalk fibres. *BioResources, 13*(1), 535–554.
[20] Laracuente, M.-L., Yu, M. H., & McHugh, K. J. (2020). Zero-order drug delivery: State of the art and future prospects. *Journal of Controlled Release, 327*, 834–856.
[21] Teong, B., Lin, C., Chang, S. J., Niu, G. C., Yao, C., Chen, I., & Kuo, S. M. (2015). Enhanced anticancer activity by curcumin-loaded hydrogel nanoparticle-derived aggregates on A549 lung adenocarcinoma cells. *Journal of Materials Science: Materials in Medicine, 26*(1).

[22] Feng, W., & Wang, Z. (2023). Tailoring the swelling-shrinkable behavior of hydrogels for biomedical applications. *Advanced Science, 10*(28).
[23] Cheng, Y., Weng, S., Yu, L., Zhu, N., Yang, M., & Yuan, Y. (2019). The role of hyperthermia in the multidisciplinary treatment of malignant tumors. *Integrative Cancer Therapies, 18*, 153473541987634.